



## Effect on the calcium carbonate scale in circulating cooling water: constant magnetic and pulsed magnetic fields

Xiao-Lei Wang<sup>a</sup>, Ju-Dong Zhao<sup>a,\*</sup>, Zhi-An Liu<sup>b</sup>, Er-Jun Zhao<sup>a</sup>, Xing Yang<sup>b</sup>, Xiao-Jue Shao<sup>b</sup>

<sup>a</sup>College of Science, Inner Mongolia University of Technology, Hohhot 010051, China, Tel. +86 15147122209, email: 745619741@qq.com (X.-L. Wang), Tel. +86-471-6576370, email: jdzhao@imut.edu.cn (J.-D. Zhao), Tel. +86-471-6575445, email: ejzhao@yahoo.com (E.-J. Zhao)

<sup>b</sup>College of Energy and Power Engineering, Inner Mongolia University of Technology, Hohhot 010051, China, Tel. +86-471-6576145, email: Lza1232003@aliyun.com (Z.-A. Liu), Tel. +86 15248078051, email: 270788680@qq.com (X. Yang), Tel. +86 18847168335, email: 349869317@qq.com (X.-J. Shao)

Received 27 July 2017; Accepted 12 July 2018

---

### ABSTRACT

The scale inhibition and the different effect on calcium carbonate scale treated by magnetic fields were studied by using a home-made equipment, which simulates circulate cooling water, similar to that of power plant in Inner Mongolia. The scale inhibition rate, water viscosity, crystal phases, calcium ion concentration, and crystal morphologies of scale samples were discussed under the pulsed magnetic field and the constant magnetic field. The effect of pulsed magnetic field is more evident than that of constant magnetic field. Treated by the pulsed magnetic field, average scale inhibition rate is up to 49.47%, and the concentration of Ca<sup>2+</sup> and water quality of viscosity slightly changes. The X-ray diffraction results confirmed that pulsed magnetic field is more advantageous to restrain the formation of scale, and makes the grain size small and the non-adherent scale loose. The results indicated that the appropriate setting of frequencies for pulsed magnetic field is very important for scale inhibition.

*Keywords:* Circulating cooling water; Constant magnetic field; Pulsed magnetic field; Adherent scale; Non-adherent scale; Concentration of Ca<sup>2+</sup>; Water viscosity

---

### 1. Introduction

The deposition of water scale is common in industrial processes and domestic equipment. In the process of circulating cooling water treatment, the scale is undesirable substance on heat transfer surfaces, reduces the heat exchange efficiency and increases flow resistance. Scale not only increases the enterprise economic losses but also reduces the equipment safety, so the heat transfer equipment undertakes the very big responsibility. Therefore, research on how to effectively control and prevent the scale on the surface of the heat transfer is very important. In order to prevent the heat transfer scaling, the traditional chemical treatment method is usually applied at present. However, the chemical method needs the high cost of the scale inhibitor, which

would increase emissions of carbon dioxide causing climate change, and can also cause secondary pollution. Thus, for the treatment of the circulating cooling water, the good efficient, low cost and no secondary pollution [1,2] method is an urgent need. Up to now, among all the considered methods, the physical treatment is a good choice, and has been extensively investigated by many groups.

The physical method, i.e. magnetic treatment, which is one of the most common methods for pollution of circulating cooling water, are gradually used in industry for preventing calcium carbonate scale [3]. Magnetic treatment becomes an alternative to chemical treatment to prevent the formation of scale in the industrial circulating cooling water [4]. The equipment of different pulse magnetic field is helpful to control the formation of calcium carbonate scale [5]. However, the mechanism is still not clear. The recent research focused on the following mechanisms: (1) precip-

---

\*Corresponding author.

itation of calcium carbonate and the main components of sediment [6–9], (2) the solution crystallization nucleation or crystal growth process [4,7,10,11], (3) magnetically modified hydration and magnetohydrodynamic (MHD) processes [12].

So far, many researchers have used magnetic field to research the crystal nucleation and growth mechanism of  $\text{CaCO}_3$  scale, which has a detrimental effect on industrial heat exchange system. Hashitani et al. [13] have found that the presence of magnetic field reduces the nucleation rate. This is in good agreement with the study of Barrett and Parsons [14], who also found that magnetic treatment delays nucleation rate; meanwhile they found that magnetic treatment sustains the growth of the pre-existing crystal, and generates an impact on memory and the formation of  $\text{CaCO}_3$ . Nevertheless, Madsen [15] have proposed that magnetic treatment increased nucleation rate and crystal growth rate. Alimi et al. [16] proposed that magnetic treatment can increase the total amount of precipitate and support the homogeneous nucleation, which mainly depends on appropriate setting for water treatment PH, water flow rate and the residence time.

In addition, Busch and Busch [17] suggested that the magnetic treatment devices create additional turbulence by constricting or altering fluid, which could further enhance the anti-scaling effect by purely mechanical means. Moreover, by changing the strength of magnetic field and water flow velocity, aragonite and calcite proportions were varied. Meanwhile, Kobe et al. [18] have systematically investigated the influence of magnetic field on the crystal form of calcium carbonate both from experiments and theories, confirmed the strong influence of the applied magnetic field on the nucleation and further crystallization of calcium carbonate in hard water. Lately, Miao et al. [19] have studied the effectiveness of calcium carbonate scale in water with constant water temperature and constant flow velocity, and found that the particle size becomes small and the crystal structure changes into loose construction using electromagnetic field treatment. Moreover, Oshitani et al. [20] suggested that the pulse and alternating magnetic field to treat the stationary sample makes the metastable structure more stable than in the steady field by using a rotational device with the pulse and commutative fields. Recently, Sohaili et al. [12] suggested that the reduced removal  $\text{CaCO}_3$  percentages on the pipe walls after magnetized treatment showed an increase in crystalline aragonite, and magneto-hydrodynamics associated with Lorentz force and magnetically modified hydration effects are the proposed mechanisms involved in  $\text{CaCO}_3$  removal. Myśliwiec et al. [21] found that the mechanism of precipitation by absorbance and conductivity measurements strongly depends on the concentration of the solutions. Although much effort has been made to explain the effect on calcium carbonate precipitation, such as changing flow velocity, temperature, solution properties and rough surface, there are still controversial for possible mechanisms. Meanwhile, most of work above mentioned were investigated in water purification, or in water with constant water temperature and constant flow velocity. However, there is little for investigating circulating cooling water of power plant with the different temperatures in different process. Therefore, it is necessary to design the experiments, and further to probe into the dominating

fouling mechanism in the considered process with different temperatures, such as simulating environment of plant. Furthermore, the effect on calcium carbonate precipitation treated by constant magnetic and variable frequency magnetic fields might be different and significant, and it was reported very little.

Motivated by above mentioned, this work studies the effect on crystallization of calcium carbonate precipitated under different operating conditions. Experiments are carried out using a home-made magnetic water processor by considering scale inhibition rate, water viscosity, crystal phases, calcium ion concentration, and crystal morphologies of scale samples. Samples of calcium carbonate are mainly composed by calcite and aragonite. The water samples are measured every four hours. The crystal form and particle-size distribution of scale samples are determined using X-ray diffraction (XRD), scanning electron microscopy (SEM). The changes of crystal morphology and particle size of scale, and the rule of water precipitation are discussed under different fields.

## 2. Experimental equipment and method

### 2.1. Magnetic field generating device

The pulse magnetic field was produced by four magnetic coils, which were fixed to the outside of PVC, and the signal generator was used to detect current signal of a pulse. The direction of magnetic field is perpendicular to that of the water flow. The parameters of magnetic coils are included as follows: diameter of enameled wire 0.47 mm, pulse length 20 mm, pulse coil radius 27.5 mm, pulse coil thickness 20 mm, core diameter of soft magnetic alloy 20 mm, core length of soft magnetic alloy 51 mm, and the best number of turns 300 turns.

In this manuscript, different magnetic fields were applied for the circulating cooling water. All the experiments were divided into three groups. The first group is the control group (untreated water) with voltage of 0 V. The second one is the experimental groups, which was treated by constant magnetic field for circulating cooling water with direct voltage of 20 V. The third one is pulsed alternating magnetic field, which were applied to circulating cooling water with voltages of 20 V and square wave frequency of 50 Hz.

The distribution of magnetic fields lines inside the magnetic water processor are shown in Fig. 1. It is well-known that the energy of the electromagnetic field is transferred to the water.

### 2.2. Experiment equipment and process

The experimental equipments and technological circulating process are shown in Fig. 2. The circulating cooling water is drawn out of the collecting tank by using water circulating pumps and delivered to the convection heat exchanger via the pulsed magnetic field water processor. Water in water tank with constant temperature flows through the shell side of the heat exchanger and exchanges the heat with the circulating cooling water. The circulating cooling water is collected in the cooling tower by pipe orifice and then flows back to the water-collecting basins.

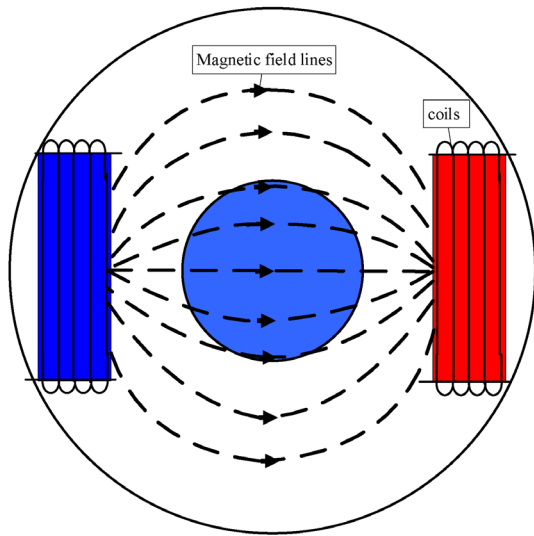


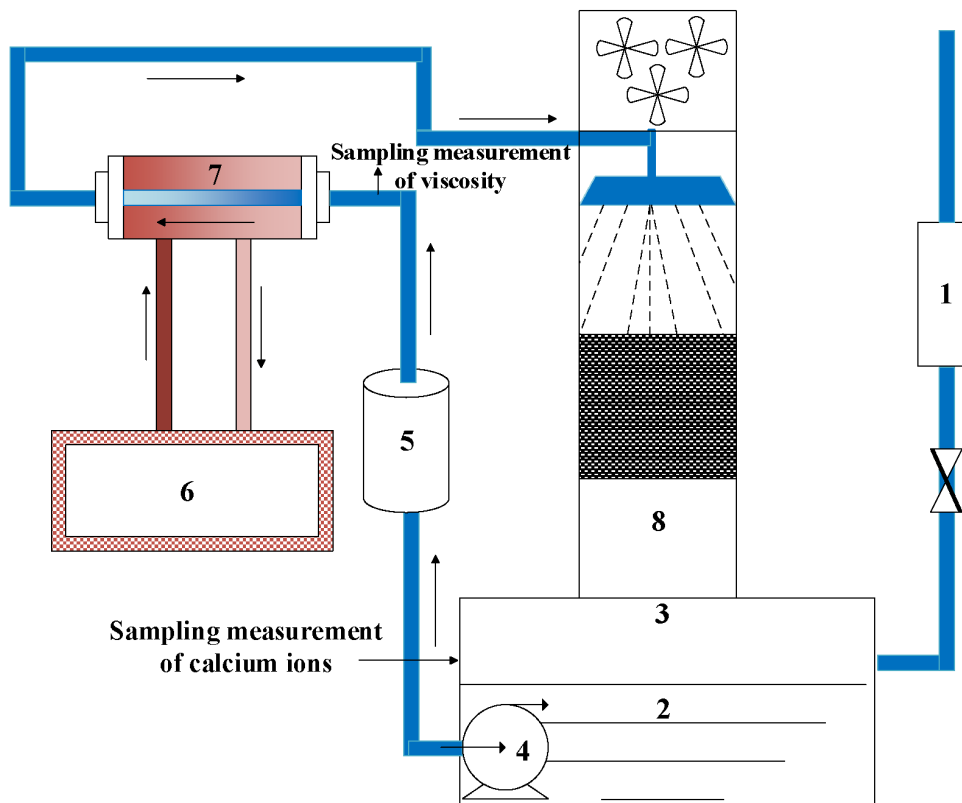
Fig. 1. The distribution of magnetic field lines inside the magnetic water process.

In the present study, three groups are considered in the study, including the control group, the constant magnetic field group, and the pulsed magnetic field group. Each experiment lasted 24 h. In the experiment process, the flow velocity of circulating cooling water is 1000 L/h, and water specifications are measured every 4 h.

The temperature of circulating cooling water is kept at  $30 \pm 0.5^\circ\text{C}$ , and the heating temperature in heat exchanger is set at  $90 \pm 0.5^\circ\text{C}$ . Due to the formation of scale in the experimental process, the concentration of  $\text{Ca}^{2+}$  and  $\text{HCO}_3^-$  is decreased. In order to maintain a stable hardness and alkalinity of circulating cooling water, pure (AR) grade (99.9%)  $\text{CaCl}_2$  was added in water with constant flow rate of 2.1 mmol/L h and AR grade  $\text{NaHCO}_3$  with constant flow rate of 2.3 mmol/L h, to compensate for the loss of  $\text{Ca}^{2+}$  and  $\text{HCO}_3^-$ , respectively.  $\text{CaCl}_2$  and  $\text{NaHCO}_3$  was purchased from Tianjin Fengchuan Chemical Reagent Technologies Co, Ltd.

2.3. Water quality index analysis

Water quality specifications, which are applied for the experiments at the beginning, are shown in Table 1,



- 1. Water supply systematic    2. Collecting tank    3. Sieve
- 4. Water circulating Pumps    5. Magnetic water processor
- 6. Constant-temperature water tank heater    7. Heat exchanger    8. Cooling Tower

Sample connection: Sampling measurement of calcium ions,  
Sampling measurement of viscosity

Fig. 2. Flow chart of anti-scaling experiment by using magnetic field water processor.

Table 1  
The initial water specification of the circulating cooling water

| Indicators   | Values |
|--|--------|
| Ca <sup>2+</sup> (mmol/L)  | 6.283  |
| Total hardness (Ca <sup>2+</sup> and Mg <sup>2+</sup> ) (mmol/L) | 10.197 |
| Alkalinity (HCO <sub>3</sub> <sup>-</sup> ) (mmol/L)             | 6.552  |
| pH   | 8.51   |
| Conductivity (μS/cm)   | 2260   |

compared with circulating cooling water quality from a power plant in Inner Mongolia. The flow chart is plotted in Fig. 2. According to DL/T502.32-2006, the water samples were taken out from collecting tank to measure calcium [Ca<sup>2+</sup>] by using the volumetric method. We take an amount of water into the viscometer, and keep constant temperature at 30°C+0.01°C, and then record standard time used in the liquid flows through the capillary volume. Water viscosity is determined by using 1835 type Ubbelohde viscometer (accuracy 0.1%). The dynamic viscosity of the circulating cooling water  $\mu$  (m·Pa·s) is calculated by using the following formula:

$$\mu = Cpt \quad (1)$$

where C (mm<sup>2</sup>/s<sup>2</sup>) is viscometer constant calibrated by standard viscosity liquid,  $\rho$  (g/cm<sup>3</sup>) is circulating cooling water density, and t (s) is the time required for standard volume liquid flows through the capillary.

#### 2.4. Acquisition and analysis of the crystal scale

During dynamic heat transfer, some CaCO<sub>3</sub> crystals deposit on the surface of containers as adherent scale, and the others are flushed away by water as non-adherent scale. The adherent scale sample was taken from the surface of heat-exchange copper tubes, while the non-adherent scale sample was taken from the sieve, whose pore diameter is  $\leq 38 \mu\text{m}$ .

After the experiment, we scraped the adherent scale from the surface of the heat exchange tubes, collected the non-adherent from the sieve, and then dried them at 105°C in the oven for 12 h. At last, we grind adherent and non-adherent scales using agate mortar, and place them in the dry bottles.

Samples for SEM images were carefully prepared so that no scratch appeared on their surfaces, and care was taken to avoid contaminating any impurities.

The D<sub>8</sub> Advance X-ray diffractometer was used to carry out the diffraction observation. The scales on the fouled tube consisted of calcite, aragonite, vaterite and their admixtures, and peak height and lattice constants (a, b, c, V) were acquired from the XRD data by using the Jade software (version 6.0). The contents of calcite and aragonite were calculated on the basis of the following formula by using the method of K value:

$$y_x = \frac{I_{X_i}}{K_A^x \sum_{i=A}^N \frac{I_i}{K_A^i}} \quad (2)$$

where  $y_x$  is the percentage of each phase, X is the X phase; i is the i phase, and  $K_A^x$  is the K value of X phase in the sample with the A phase as an internal standard substance.  $I_{X_i}$  is the integrated intensity of X phase with the A phase as an internal standard substance, and  $K_A^i$  is the K value of i phase in the sample with the A phase as an internal standard substance. K is 3.12 for calcite, and K is 1.13 for aragonite.

#### 2.5. Average scale inhibition rate $\eta$

According to the thermal equilibrium conditions of heat transfer theory [22], total heat transfer coefficient M is calculated by using the following formula:

$$M = \frac{m_c c_{pc} (T_1 - T_2) \ln \left( \frac{T_3 - T_2}{T_4 - T_1} \right)}{A [(T_3 - T_2) - (T_4 - T_1)]} \quad (3)$$

where  $T_1$ (K) and  $T_2$ (K) are the inlet and outlet temperatures of circulating cooling water,  $T_3$ (K) and  $T_4$ (K) are the inlet and outlet temperatures of the heated water, respectively. A (m<sup>2</sup>) is the total heat transfer area,  $m_c$  (kg/s) is the mass velocity, and  $c_{pc}$  [J/(kg·K)] is specific heat at the constant pressure.

The fouling resistance is then defined by the following formula:

$$R_f = \frac{1}{M_t} - \frac{1}{M_{t=0}} \quad (4)$$

where  $R_f$  [(m<sup>2</sup>·K)/W] is the fouling resistance at time t,  $M_t$  [W/(m<sup>2</sup>·K)] is the total transfer coefficient at the time t, and  $M_{t=0}$  is the total transfer coefficient at the initial time. The scale inhibition rate  $\eta$  can be obtained through the computer every ten minutes by fouling resistance in the experimental groups and the control group:

$$\eta_t = \left[ 1 - \frac{R_{\text{experimental}}(t)}{R_{\text{control}}(t)} \right] \times 100\% \quad (5)$$

where  $R_{\text{experimental}}(t)$  [(m<sup>2</sup>·K)/W] is the fouling resistance of the treated water, and  $R_{\text{control}}(t)$  is the fouling resistance of untreated water (the control group).

The average scale inhibition rate  $\eta$  can be obtained by the following formula:

$$\eta = \frac{\sum_{i=1}^N \eta_i}{N} \quad (6)$$

#### 2.6. The scale inhibition rate $\eta'$ by using weight method

For the test, the scale inhibition rate by using weight method is calculated by using the gravimetric method as below:

$$\eta' = \left( 1 - \frac{m_1}{m_2} \right) \times 100\% \quad (7)$$

where  $m_1$ (g) is the weight of adherent scale in the experiment group, and  $m_2$ (g) is the weights of adherent scale in the control group.

### 3. Results and discussion

#### 3.1. Analysis of scale inhibition rate by using fouling resistance method and weight method

Scale inhibition rate is a macroscopic characterization, which reflects the differences of the convection heat exchange coefficients between the experimental groups and control group.  $T_1, T_2, T_3, T_4$  can be collected by automatic temperature acquisition system in the experimental groups and the control group, as illustrated by Figs. 3, 4. Scale inhibition rate of fouling resistance  $\eta$  can be obtained through the computer every ten minutes. Average scale inhibition rate  $\eta_t$  was obtained by Eq. (6). Scale inhibition rate depends on the generation amount of adherent scale using weight method, so scale inhibition rate  $\eta$  was obtained by Eq. (7). Average scale inhibition rate  $\eta_t$  and scale inhibition rate  $\eta$  are shown in Table 2. For the control group, the adherent scale quantity is 7.608 g. For the constant magnetic group, average scale inhibition rate  $\eta_t$  and scale inhibition rate  $\eta$  are negative. The adherent scale quantity increases with the value of 8.413

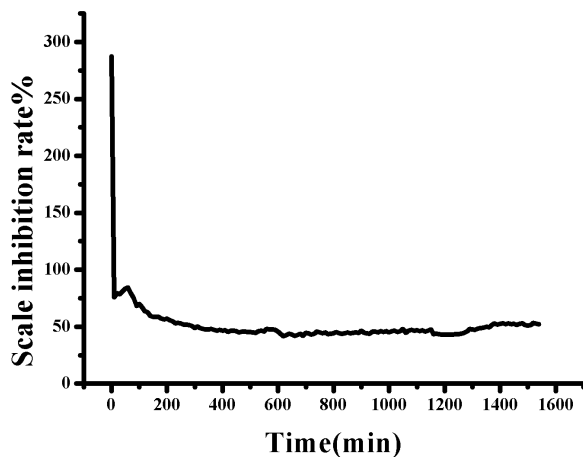


Fig. 3. The calculated scale inhibition rate-time curve by using fouling resistance method under constant magnetic field.

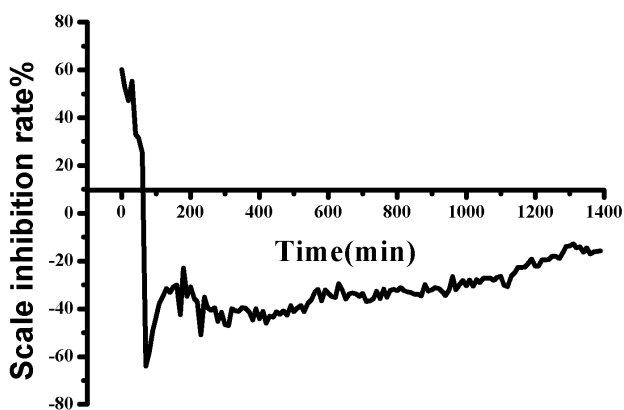


Fig. 4. The calculated scale inhibition rate-time curve by using fouling resistance method under pulsed magnetic field.

g, compared with that of control group. This indicated that the constant magnetic field promotes the formation of the adherent scale, which is also observed by previous investigation [23]. From Fig. 3 it is clearly seen that scale inhibition rate increases with the increase of time by using fouling resistance method. This suggested that the shorter the duration under the constant magnetic field lasted, the more favorable for the formation of scale-was. From Table 2, for the pulsed magnetic group, average scale inhibition rate  $\eta$  and scale inhibition rate  $\eta'$  are 49.47% and 21.46%, respectively. It is obvious to present that the pulsed magnetic field restrains the formation of the adherent scale. This is confirmed by Guo et al. [24]. Moreover, as illustrated by Fig. 4, scale inhibition rate of fouling resistance is stable and positive in the whole time under pulsed magnetic field, to inhibit scale formation. Therefore, these experimental data give evidence that the pulsed magnetic field can restrain the formation of the adherent scale to achieve the goal of scale removal.

#### 3.2. The concentration of $Ca^{2+}$ analysis

In the experiments, the concentration of  $Ca^{2+}$  was kept as a constant by the water supply system. The change of  $Ca^{2+}$  concentration is closely related to scale quantity. This can be explained from Eq. (8), which is as follows:



Fig. 5 shows that the concentration of  $Ca^{2+}$  changes with time under constant magnetic and pulsed magnetic fields. In the control group, the concentration of  $Ca^{2+}$  is small downward trend, due to the formation of adherent scale. For the constant magnetic group, the concentration of  $Ca^{2+}$  is bigger downward trend than that for the control group, which is in good agreement with more adherent scale for the constant magnetic group compared with that for the control group. This was also observed by Highashitani et al. [13]. For the pulsed magnetic field group, the average concentration of  $Ca^{2+}$  changes slightly in all the circulating process, and total scale quantity (28.880 g) is less than that (74.390 g) for control group, because the adherent scale quantity is the least among all the groups. This indicates that the pulsed magnetic field restrains the formation of  $CaCO_3$  scale, which is also suggested by Guo et al. [24].

Table 2

The adherent scale quantity, average scale inhibition rate ( $\eta$ ) and scale inhibition rate ( $\eta'$ ) by using weight method

|                             | Adherent scale quantity (g) | Average scale inhibition rate $\eta$ | Scale inhibition rate using weight method $\eta'$ |
|-----------------------------|-----------------------------|--------------------------------------|---|
| The control group           | 7.608                       | 0                                    | 0   |
| The constant magnetic group | 8.413                       | -28.29                               | -10.5   |
| The pulsed magnetic group   | 5.975                       | 49.47                                | 21.46   |



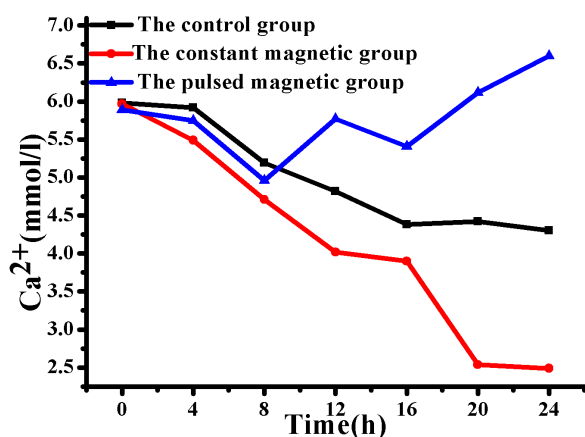


Fig. 5. The concentration of Ca<sup>2+</sup> statistics for the control group and experimental groups.

### 3.3. Viscosity of water change

During the experiments, not only is the concentration of Ca<sup>2+</sup> changed, but also the water viscosity is changed. In this study, water samples were taken out from the after processor and the water viscosity was measured. The formed non-adherent scale is always addressed as bulk fluid, which was intercepted by sieve. Generally, the bulk fluid increasing resulted in the increasing of the water viscosity in circulating cooling water. From Fig. 6, it is interesting to note that the water viscosity for constant magnetic group tends to increase with the increase of time, which is similar to that for the control group. The water viscosity for constant magnetic group is larger than that for control group, which is in good agreement with the change of Ca<sup>2+</sup> concentration. For pulsed magnetic group, the water viscosity tends to decrease, because the non-adherent scale quantity greatly decreases. These results can be explained by the theory of Eyring [25]. Hence, the pulsed magnetic can reduce the water viscosity and inhibit the formation of non-adherent scale. The reason for reducing of viscosity might be that water in this study with Ca<sup>2+</sup>, Na<sup>+</sup>, HCO<sub>3</sub><sup>-</sup> and Cl<sup>-</sup>, can be seen as magnetoelastoelectric medium, and polarization loss and magnetization loss will occur under the action of the alternating magnetic field. The alternating magnetic field is accompanied by alternating electric field. This can lead to the increase of kinetic energy and reduce the activity energy of water. Then, the viscosity of water decreases.

### 3.4. Identify phase spectrum of CaCO<sub>3</sub> scale samples

There are three different crystal polymorphs of calcium carbonate (CaCO<sub>3</sub>). It is well-known that calcite is the most stable under ambient conditions, aragonite is the high-pressure polymorph, and vaterite is thermodynamically unstable [3,26–29]. In order to measure the composition of crystalline phases, XRD were carried out for scale sample. Among all the samples, vaterite was not detected, so only the compositions of calcite and aragonite were listed in Table 3. It is interesting to note that mass fraction of aragonite in adherent scale is more than that in non-adherent

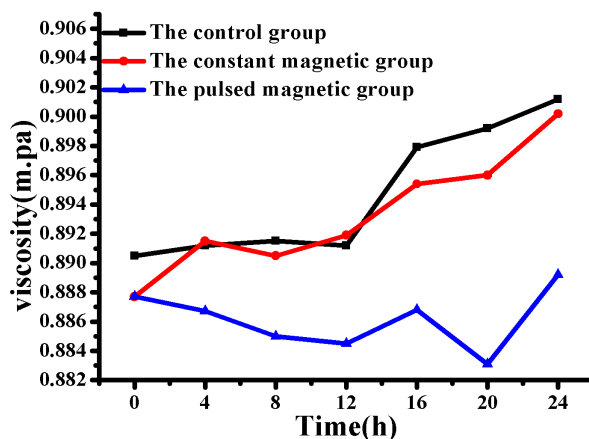


Fig. 6. The water viscosity for the control group and experimental groups.

Table 3

The content of aragonite and calcite

|                             | Quantity fraction $y_i$ % |         |                    |         |
|-----------------------------|---------------------------|---------|--------------------|---------|
|                             | Adherent scale            |         | Non-adherent scale |         |
|                             | Aragonite                 | Calcite | Aragonite          | Calcite |
| The control group           | 98.10                     | 1.90    | 82.15              | 17.85   |
| The constant magnetic group | 98.23                     | 1.77    | 69.88              | 30.12   |
| The pulsed magnetic group   | 95.97                     | 4.03    | 54.32              | 45.68   |

one, while mass fraction of calcite is opposite. From Table 3, it is obvious to notice that the adherent scale is mostly composed of aragonite, whose mass fraction exceeds 95%. In non-adherent scale, quantity of aragonite for experimental groups is larger than that for the control group, and quantity of calcite is opposite. These indicate that magnetic field has little effect on compositions of adherent scale, though it has obvious influence on that of non-adherent one. For pulsed magnetic groups, fractions of aragonite and calcite are very close in non-adherent scale.

### 3.5. CaCO<sub>3</sub> scale morphology analysis

The SEM images magnified 2000× and 10000× are plotted in Figs. 7–9. It is well known that aragonite is needle, and calcite is block. From Fig. 7 for the control group, it is obvious to see that the adherent and non-adherent scales are composed of almost all aragonite and a little calcite, which is consistent with that the composition of scale is mostly aragonite from XRD results. From Figs. 8b and 8d, it is interesting to note that there are some calcite crystals in non-adherent scale for the constant magnetic group. This agrees with that there are 30.12% calcite in non-adherent scale from XRD results. For the pulsed magnetic group, the grain size is smaller and looser than that for the control group. From Figs. 7–9, it is evident to see that the

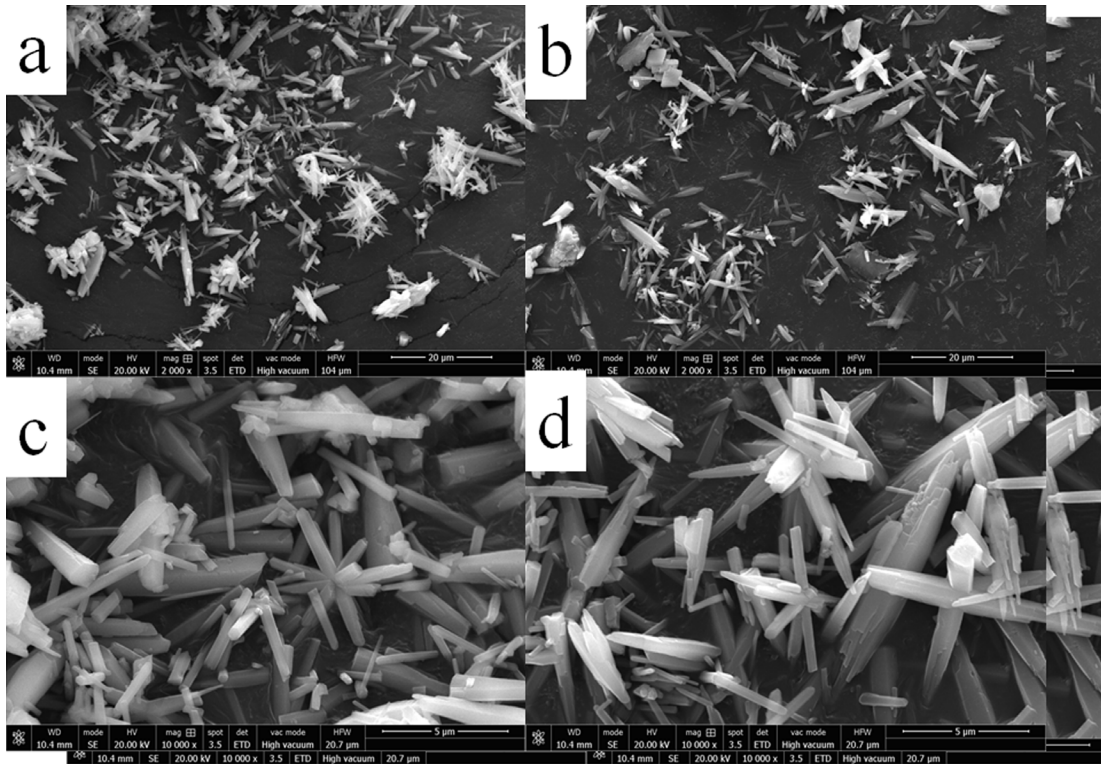


Fig. 7. SEM images for the control group, a is 2000× Adherent scale, b is 2000× Non-adherent scale, c is 10000× Adherent scale, d is 10000× Non-adherent scale.

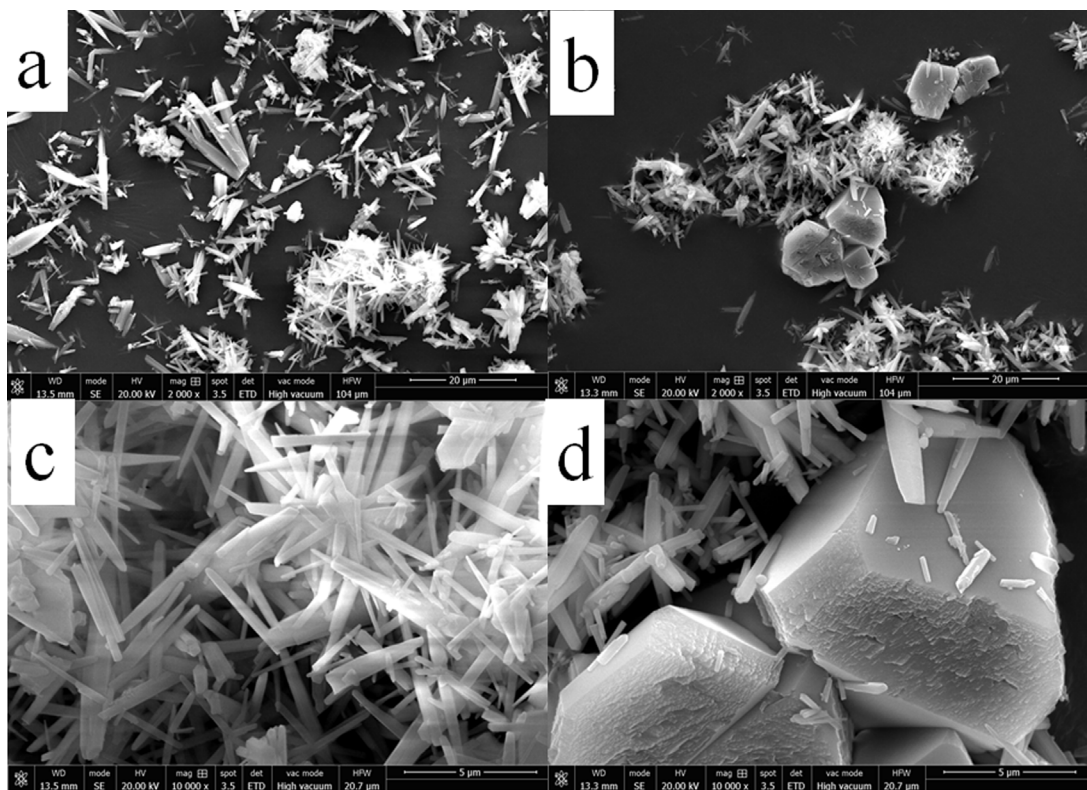


Fig. 8. SEM images for the constant magnetic group, a is 2000× Adherent scale, b is 2000× Non-adherent scale, c is 10000× Adherent scale, d is 10000× Non-adherent scale.



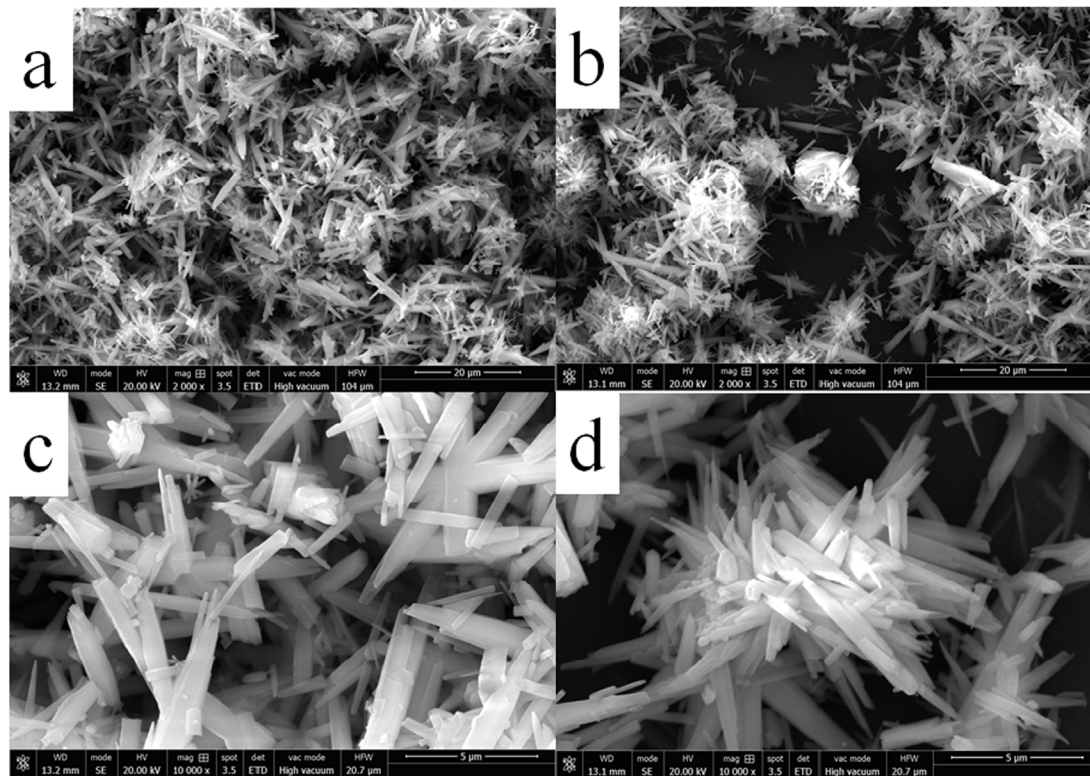


Fig. 9. SEM images for the pulsed magnetic group, a is 2000× Adherent scale, b is 2000× Non-adherent scale, c is 10000× Adherent scale, d is 10000× Non-adherent scale.

particle size of adherent scale is larger than that of non-adherent one, and the former is looser than the latter. It is also obvious to see that particle size treated by magnetic field (Figs. 8 and 9) is larger than that of control group (Fig. 7), and the particles in Figs. 8 and 9 tend to coagulate than that in Fig. 7. This may be due to that magnetic field neutralized the surface of particles and caused the shifting of ions from the bulk solution towards the particle surface, which leads to that the larger particles are less likely to adhere to the pipe walls [12].

#### 4. Conclusion

The influence on the calcium carbonate scale for constant magnetic field and pulsed magnetic field in circulating cooling water were investigated by using the self-made equipment. The scale inhibition rate, water viscosity, crystal phases, calcium ion concentration, and crystal morphologies of scale samples were discussed under the different conditions, e.g. the pulsed magnetic and the constant magnetic fields. For the constant group, the formed scale leads to the decrease of the concentration of  $\text{Ca}^{2+}$  and the increase of the water viscosity. While for pulsed magnetic group, the formation of scaled were restrained, and scale inhibition rates are positive, which is in good agreement with the slight change of the concentration of  $\text{Ca}^{2+}$  and the slight change of the water viscosity. These results are also confirmed by previous experiments. Moreover, the grain size treated by pulsed magnetic field is smaller and looser

than those treated without magnetic field and with constant magnetic one. It can be concluded that the pulsed magnetic field might be one of good physical methods to treat the circulating cooling water, in order to scale removal from convection heat-exchanger.

#### Acknowledgments

This project was supported by National Natural Science Foundation of China (61761036, 51268040, 51068020).

#### References

- [1] L. Jiang, J. Zhang, D. Li, Effects of permanent magnetic field on calcium carbonate scaling of circulating water, *Desal. Water Treat.*, 53 (2013) 1–11.
- [2] A. Fathi, T. Mohamed, G. Claude, G. Maurin, B.A. Mohamed, Effect of a magnetic water treatment on homogeneous and heterogeneous precipitation of calcium carbonate, *Water Res.*, 40 (2006) 1941–1950.
- [3] L.D. Tijjing, D.H. Lee, D.W. Kim, D.W. Kim, Y.I. Cho, C.S. Kim, Effect of high-frequency electric fields on calcium carbonate scaling, *Desalination*, 279 (2011) 47–53.
- [4] E.J.L. Toledo, T.C. Ramalho, Z.M. Magriotis, Influence of magnetic field on physical–chemical properties of the liquid water: Insights from experimental and theoretical models, *J. Mol. Struct.*, 888 (2008) 409–415.
- [5] L. Holysz, M. Chibowski, E. Chibowski, Time-dependent changes of zeta potential and other parameters of in situ calcium carbonate due to magnetic field treatment, *Colloids Surf. A.*, 208 (2002) 231–240.



- [6] X. Xing, Research on the electromagnetic anti-fouling technology for heat transfer enhancement, *Appl. Therm. Eng.*, 28 (2008) 889–894.
- [7] F. Alimi, M. Tlili, M.B. Amor, C. Gabrielli, G. Maurin, Influence of magnetic field on calcium carbonate precipitation, *Desalination*, 206 (2007) 163–168.
- [8] D. Beruto, M. Giordani, Calcite and aragonite formation from aqueous calcium hydrogen carbonate solutions: effect of induced electromagnetic field on the activity of  $\text{CaCO}_3$  nuclei precursors, *J. Chem. Soc. Faraday Trans.*, 89 (1993) 2457–2461.
- [9] E. Chibowski, L. Hołysz, A. Szcześ, M. Chibowski, Precipitation of calcium carbonate from magnetically treated sodium carbonate solution, *Colloids Surf. A.*, 225 (2003) 63–73.
- [10] S. Knez, C. Pohar, The magnetic field influence on the polymorph composition of  $\text{CaCO}_3$  precipitated from carbonized aqueous solutions, *J. Colloid Interf. Sci.*, 281 (2005) 377–388.
- [11] M. Morimitsu, K. Shiomi, M. Matsunaga, Magnetic effects on Alkyl ammonium chloride solutions investigated by interfacial tension measurements at the mercury/solution interface, *J. Colloid Interf. Sci.*, 229 (2000) 641–643.
- [12] J. Sohaili, H.S. Shi, Lavania-Baloo, N.H. Zardari, N. Ahmad, S.K. Muniyandi, Removal of scale deposition on pipe walls by using magnetic field treatment and the effects of magnetic strength, *J. Clean. Prod.*, 139 (2016) 1393–1399.
- [13] K. Higashitani, A. Kage, S. Katamura, K. Imai, S. Hatade, Effects of a magnetic field on the formation of  $\text{CaCO}_3$  Particles, *J. Colloid Interf. Sci.*, 156 (1993) 90–95.
- [14] R.A. Barrett, S.A. Parsons, The influence of magnetic fields on calcium carbonate precipitation, *Water Res.*, 32 (1998) 609–612.
- [15] H.E.L. Madsen, Crystallization of calcium carbonate in magnetic field in ordinary and heavy water, *J. Cryst. Growth*, 267 (2004) 251–255.
- [16] F. Alimi, M. Tlili, M.B. Amor, C. Gabrielli, G. Maurin, Influence of magnetic field on calcium carbonate precipitation, *Desalination*, 206 (2007) 163–168.
- [17] K.W. Busch, M.A. Busch, Laboratory studies on magnetic water treatment and their relationship to a possible mechanism for scale reduction, *Desalination*, 109 (1997) 131–148.
- [18] S. Kobe, G. Drazic, A.C. Cefalas, E. Sarantopoulou, J. Strazisar, Nucleation and crystallization of  $\text{CaCO}_3$  in applied magnetic fields, *Cryst. Eng.*, 5 (2002) 243–253.
- [19] X. Miao, L. Xiong, J. Chen, Z. Yang, W. He, Experimental study on calcium carbonate precipitation using electromagnetic field treatment, *Water Sci. Technol.*, 67 (2013) 2784–2790.
- [20] J. Oshitani, R. Uehara, K. Higashitani, Magnetic effects on electrolyte solutions in pulse and alternating fields, *J. Colloid-Interf. Sci.*, 209 (1999) 374–379.
- [21] D. Myśliwiec, A. Szcześ, S. Chibowski, Influence of static magnetic field on the kinetics of calcium carbonate formation, *J. Ind. Eng. Chem.*, 35 (2016) 400–407.
- [22] J.D. Zhao, Z.A. Liu, E.J. Zhao, Combined effect of constant high voltage electrostatic field and variable frequency pulsed electromagnetic field on the morphology of calcium carbonate scale in circulating cooling water systems, *Water Sci. Technol.*, 70 (2014) 1074–1082.
- [23] A. Fathi, T. Mohamed, G. Claude, G. Maurin, B.A. Mohamed, Effect of a magnetic water treatment on homogeneous and heterogeneous precipitation of calcium carbonate, *Water Res.*, 40 (2006) 1941–1950.
- [24] L. Xiong, J. Li, G. Hu, J. Chen, G. Lin, W. He, Design of a bipolar magnetic pulse generator and experimental study on its anti-scaling effect, *High Voltage Eng.*, 41 (2015) 2008–2014.
- [25] G. Han, Z. Fang, M. Chen, Modified Eyring viscosity equation and calculation of activation energy based on the liquid quasi-lattice model, *Sci. China Phys. Mech.*, 53 (2010) 1853–1860.
- [26] H. Colfen, Precipitation of carbonates: recent progress in controlled production of complex shapes, *Curr. Opin. Colloid In.*, 8 (2003) 23–31.
- [27] Z.D. Nan, X.N. Chen, Q.Q. Yang, X.Z. Wang, Z.Y. Shi, W.G. Hou, Structure transition from aragonite to vaterite and calcite by the assistance of SDBS, *J. Colloid Interf. Sci.*, 325 (2008) 331–336.
- [28] A.L. Boettcher, P.J. Wyllie, The Calcite-Aragonite transition-measured in the system, *J. Geol.*, 76 (1968) 314–330.
- [29] Z.D. Nan, Z.Y. Shi, M. Qin, W.G. Hou, Z.C. Tan, Formation process and thermodynamic properties of calcite, *Chin. J. Chem.*, 25 (2007) 592–595.